ECOLOGICAL MODELLING 197 (2006) 221–236

available at www.sciencedirect.com

SCIENCE DIRECT®

journal homepage: www.elsevier.com/locate/ecolmodel

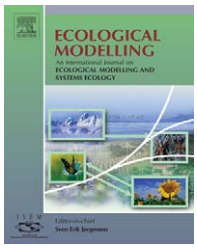

Modeling the spread of the Emerald Ash Borer

Todd K. BenDor[a,*], *Sara S. Metcalf*[b], *Lauren E. Fontenot*[b], *Brandi Sangunett*[c], *Bruce Hannon*[b]

[a] *Department of Urban and Regional Planning, University of Illinois, 111 Temple Buell Hall, 611 Taft Drive, Champaign, IL 61820, United States*

[b] *Department of Geography, University of Illinois, Urbana, IL 61801, United States*

[c] *Department of Natural Resources and Environmental Sciences, University of Illinois, Urbana, IL 61801, United States*

ARTICLE INFO

Article history:
Received 17 April 2005
Received in revised form 16 February 2006
Accepted 3 March 2006
Published on line 18 April 2006

Keywords:
Spatial modeling
Cellular automata
Dynamic modeling
Invasive species
Emerald ash borer (*Agrilus planipennis*)
Spatially explicit modeling
Spatial dispersion
Ash trees (*Fraxinus* spp.)

ABSTRACT

Recently, an invasive Asian beetle known as the Emerald Ash Borer (EAB) (*Agrilus planipennis* Coleoptera: Buprestidae) has emerged as a threat to ash trees in the Midwestern United States and Canada [McCullough, D.G., Katovich, S.A., 2004. Pest Alert: Emerald Ash Borer. United States Forest Service, Northeastern Area. NA-PR-02-04]. Significant infestations in Michigan and nearby areas have all but doomed nearly 1 billion native ash trees. However, surrounding regions may still be able to prevent tree damage from occurring at the scale once inflicted by Dutch elm disease in the 1970s. This paper presents an argument for the establishment of a widely accessible knowledgebase of information on the EABs spread capabilities. We argue that spatial dynamic modeling stands as a flexible and powerful decision support system platform. We present initial simulations of EAB spread scenarios constructed using tree information and land use data collected for DuPage County, IL, an uninfected suburban county in the Chicago metropolitan area. These simulations test policies focused on impeding the costly spread of the beetle. This analysis also presents a framework for further studies assessing the economic impacts on municipalities and counties due to tree removal costs and aesthetic damage. Our work points to human driven movement as the major vector for EAB spread throughout our study area. Here, the focus falls on the ability of state and county implemented firewood quarantines to act as effective policies for slowing EAB spread.

1. Introduction

During the summer of 2002, officials with the Michigan Department of Agriculture Pesticide and Plant Pest Management Division and the U.S. Department of Agriculture (USDA) Animal and Plant Health Inspection Service (APHIS) announced the discovery of a newly-introduced exotic-invasive Asian beetle known as the Emerald Ash Borer (EAB) (*Agrilus planipennis* Coleoptera: Buprestidae). By the time the announcement was made, the EAB had already spread throughout five southeast Michigan counties (Bauer et al., 2003a). Although firewood quarantines have been mandated in Michigan and nearby areas in Ontario, Canada, reports of EAB spread through wood products such as nursery stock and firewood into Ohio, Indiana, Maryland, and Virginia (McCullough and Katovich, 2004), have belied the efficacy of these quarantine policies.

The economic and environmental impacts of the EAB have been acutely felt in southeastern Michigan where officials have already found fatal damage to the interior cambium

* *Corresponding author*. Tel.: +1 217 333 5172; fax: +1 217 244 1717.
E-mail address: bendor@uiuc.edu (T.K. BenDor).

0304-3800/$ – see front matter © 2006 Elsevier B.V. All rights reserved.
doi:10.1016/j.ecolmodel.2006.03.003

circulatory systems of over 6 million green (*Fraxinus pennsylvanica*), black (*F. nigra*), and white (*F. americana*) ash trees (McCullough and Katovich, 2004). Various spread scenarios anticipate deaths of up to 700 million trees. Although it is anticipated that the EAB will be responsible for the death of a major portion of over 700 million susceptible ash trees in Michigan, the effects on property values and municipal budgets due to tree-felling and replanting efforts (Herms et al., 2004) in the wake of impending declines in mature tree stands have yet to be studied in any depth. While the EAB has proven itself to be a destructive pest, capable of destroying vast amounts of natural capital in the economies of the upper Midwest, research focused specifically on the flight and spread characteristics of the EAB has been limited (Brown-Rytlewski and Wilson, 2003; Haack and Petrice, 2003; McCullough et al., 2003; Bauer et al., 2003b).

This framework for an integrated decision support system will prove itself essential in developing detailed studies that assess and predict patterns in damage to tree populations, and the accompanying economic and environmental impacts. No such framework has been developed that is explicit in both space and time for the compilation of spatial spread information for the Emerald Ash Borer.[1]

The purpose of this paper is to describe how an innovative collaborative modeling approach was used to create a spatially dynamic model of EAB spread in DuPage County, IL, an uninfected suburban county in the Chicago metropolitan area (Fig. 1). Using the collaborative modeling environment pioneered by Maxwell and Costanza (1997), we were able to formulate a dynamic model to serve as a decision support system for data collected through interviews with experts as well as exploration of pertinent entomology and dendrology literature. This article will demonstrate the usefulness of spatio-temporal modeling as a framework for rapid knowledge dissemination and actualization with the goal of studying the mechanisms responsible for the EABs invasive spread dynamics.

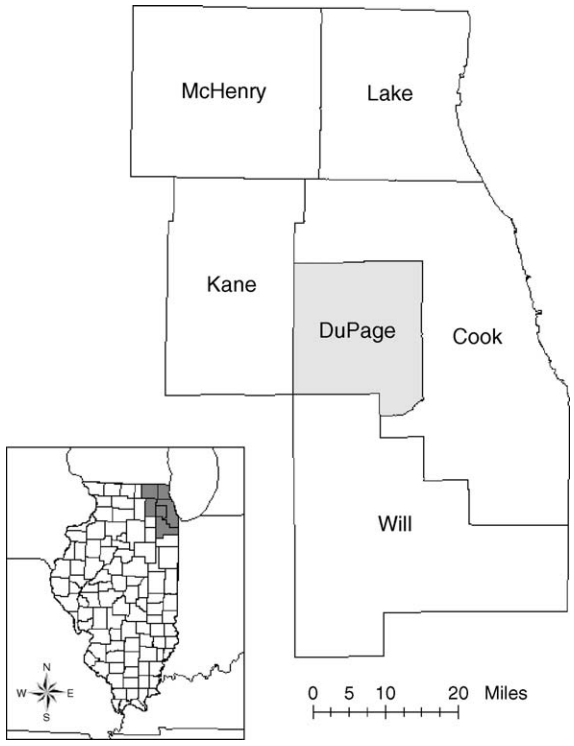

Fig. 1 – The Chicago metropolitan region and the DuPage County, IL study area.

2. Background

2.1. *Biology of the Emerald Ash Borer*

The larval instars of the EAB feed upon the inner bark and outer sapwood (cambium) of ash trees. Due to the important role of the cambium in vital nutrient transport functions, EAB infestations commonly have the effect of girdling trees, an injury that is almost always fatal. The EABs life cycle spans 1 year (Fig. 2) (Bauer et al., 2003a), although evidence of 2 or even 3-year life cycles exists (Wilson, 2004). Adults lay eggs from late May to early August in the trunks of trees that are at least 2 in. in diameter (Brown-Rytlewski and Wilson, 2003). The eggs hatch after a week, and the larvae begin consuming the inner bark and outer sapwood of the host trees until October (Lyons et al., 2003). The larvae then enter a dormant state spending the winter in their feeding galleries until they pupate in spring (Bauer et al., 2003a). The adult beetles emerge in May and live 2–3 weeks, just long enough to mate and lay eggs (Lyons et al., 2003). As is the case for most insects, life stage transitions are temperature dependent, such that specific dates of emergence vary from year to year. Females usually lay 60–90 eggs in their lifetime (McCullough and Katovich, 2004), though fecundity is highly variable (Lyons et al., 2003).

The eggs are extremely small, and larvae remain hidden by the bark making visual detection nearly impossible. The earliest indications of the insect are the presence of D-shaped exit holes created by adults as they emerge through the bark. Thus, identification is delayed by at least 1 year of initial infestation. After 2 years of infestation, canopy dieback of 30–50% is often visible. On average, it has been observed that the EAB can fatally injure an ash tree within 3–4 years of initial infestation (McCullough and Katovich, 2004).

Due to the recent discovery of this insect, many aspects of the EABs life cycle are still unknown. In such cases, we relied upon the best available professional knowledge of wood boring beetles.[2]

[1] Researchers studying other invasive species have created knowledge base systems allowing for the compilation of significant data on species spread capabilities and behavior. An example of this is the decision-support system created at Virginia Tech for the USDA funded National Slow the Spread of the Gypsy Moth Project (http://www.da.ento.vt.edu/). This system has vastly expanded the abilities of researchers to catalog current behavior and model the spatial spread of the Gypsy Moth through time and space.

[2] Some of this information came from insects such as the Bronze Birch Borer (*Agrilus anxius* Gory), as well as a host of other wood boring beetles (Barter, 1957; Haack and Poland, 2002; Auclair et al., 2005; Smith and Hurley, 2000).

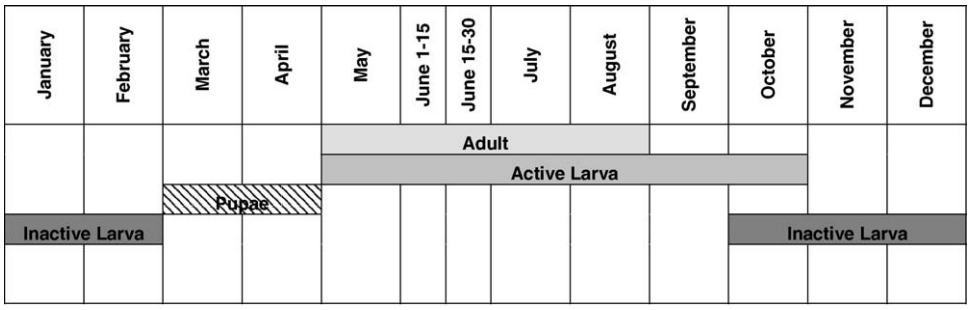

Fig. 2 – Diagram of Emerald Ash Borer lifecycle. Source: Lyons et al. (2003) and Bauer et al. (2003a).

2.2. *Biology of host trees—Fraxinus species*

Emerald Ash Borer infestations in the United States and Canada have largely claimed trees in the genus *Fraxinus*, particularly white ash (*F. americana*), green ash (*F. pennsylvanica*), and black ash (*F. nigra*) (Haack et al., 2002). These species tend to be rapidly growing, shade tolerant trees that colonize gaps in forests and old fields. The EABs rapid spatial spread has been attributed to the fact that virtually all ash species have been planted to some extent for landscaping practices in both private and public settings. Ashes can comprise 15–20% of the street trees in many areas in Michigan, and up to 15–20% of the catalogued street trees in the Chicago region (Nowak, 1994; Chicago Bureau of Forestry, 1995; McPherson et al., 1997).

Black ash (*F. nigra*) is a common shade intolerant hardwood species found in lowlands within the upper-Midwestern United States (Erdmann et al., 1987). Growing mainly on organic peats and mucks, this species typically attains heights of 9–13 m (30–45 ft) after 50 years, and 15–18 m (50–60 ft) at 100 years of age (Levy, 1970). The largest *F. nigra* individuals have been found with a diameter at breast height (DBH) of 25 cm (10 in.) at 110 years and 30 cm (12 in.) at 130 years of age (Erdmann et al., 1987). Black ash trees, like other *Fraxinus* spp. tend to have intervals of large seed crop production, with mast seed crops occurring in 1–8 year intervals (Erdmann et al., 1987; Burns and Honkala, 1990). Black ash flowering occurs in May and June, often concurrent with leaf emergence (Burns and Honkala, 1990). Fruit ripening occurs between June and September, with seed dispersal occurring between July and October (Williams, 1936; Wang, 1974). White ash (*F. americana*) is a dominant deciduous tree found throughout the upper Midwestern United States (Vines, 1960). White ash is particularly susceptible to several natural and anthropogenically produced pathogens such as ash decline (also known as ash yellows), a pathogen thought to be the result of either acid deposition or various fungi or viral infections (Hibben and Silverborg, 1978; Millers et al., 1989). These *F. Americana* individuals often obtain heights between 60 and 70 ft (18–21 m) (Hosie, 1969) and experience flowering between April and May, with seed dispersal between August and November (Vines, 1960; Bjorkbom, 1979; Schlesinger, 1990). Green Ash (*F. pennsylvanica*) can grow up to 20 m (66 ft) high with diameters of 46–61 cm (1.5–2 ft). This flood-tolerant species is almost completely confined to bottomland sites, but grows well when planted on moist upland soils (Wright, 1959).

We utilize these assumptions about the processes and functions occurring within each species' population to construct a spatio-temporal model of the EABs spread. The following section details our techniques for the model construction.

3. Methods

3.1. *Collaborative framework and theory*

Interactions that have been responsible for the rapid spread of the EAB are complicated not only because they simultaneously involve various components (including environmental stochasticity, ash population dynamics, and EAB carrying capacity considerations among others), but also because these components interact dynamically to create system delays and complex feedback effects. Long-term studies or experimental manipulations are often infeasible in complex ecological and economic systems, especially when information is needed quickly. Representative models can help to fill knowledge gaps and assist in decision-making and policy-forming activities as well as act as a knowledgebase for subsequent empirical data gathering efforts (Costanza and Voinov, 2001).

Hall and Day (1977) consider three specific perceptual uses of modeling: understanding, assessing, and optimizing. In the case of the EAB, a spatial model of the insect can be used to gain a more rigorous understanding of the mechanisms governing species spread. In a number of cases, including this one, models of this type are generated before significant field or laboratory studies have been completed. Here, the focus of the modeling process falls primarily on examining the features seen to be the most critical in determining the behavior of the study system (Costanza and Voinov, 2001). After empirical measurements and data are gathered, models can be used to test system assumptions.

3.2. *Adding spatial dimensions to models*

The last five decades have seen significant developments in the field of system dynamics, an approach to simulation modeling that consists of dynamic models that explicitly consider information feedbacks that govern the interactions of a system. The capabilities of this particular technique have proven to be very useful in aiding analysis and policy decisions in

management, social and scientific systems (Forrester, 1969, 1972; Ford, 1999; Sterman, 2000; Guo et al., 2001).

One advantage of this simulation-modeling paradigm is the non-technical manner in which models can be communicated. By creating an environment where the user is not concerned with many of the highly technical and mathematical aspects of modeling, the possibility of using system dynamics as an educational tool has vastly increased (Costanza and Voinov, 2001). The use of the stock-flow-feedback relationship as a means for describing models that exist on top of a mathematical framework allows these models to be understood by non-technically oriented individuals. This facet of the system dynamics methodology sets it apart significantly from the abstract rules of spatially arrayed cellular automata (CA) as well as other types of mathematical approaches to simulation modeling (see Ford (1999) and Sterman (2000) for more information on the system dynamics methodology, and Wolfram (1994) for more information on CA modeling).

However, system dynamics models have encountered limitations in modeling spatial systems (Ford, 1999). The historical trend in the system dynamics methodology has been to use aggregate figures for a region. In many situations however, there exists a setting where environmental heterogeneity significantly impacts the system behavior. Here, spatio-temporal modeling is essential (Maxwell and Costanza, 1997; Deal et al., 2004). Spatial models become necessary for developing a realistic description of past system behavior in environments were non-uniformity is pervasive and landscape changes have major effects on the behavior of the system of interest.

We utilize the spatial modeling environment (SME) developed at the University of Maryland (continued at the University of Vermont) as a template for achieving balance between accessibility and functional usefulness in creating a spatially explicit model of the EAB spread. SME has attempted to address the tendency of the current generation of simulation models to be idiosyncratic, and comprehensible only to their creators (Acock and Reynolds, 1990; Fall and Fall, 2001). Since the communication of the structure of an incomprehensible model to others can be a major obstacle to its acceptance, a popular method of reducing complexity has been the use of graphical, icon-based interfaces. Here, model structure is represented in a way that allows new users to recognize, understand, and critique major interactions easily (Maxwell and Costanza, 1997; Voinov et al., 1999). The advances in usability that this simulation modeling system presents allow spatial models that are created, tested and run using a collaborative process to become consensus-building tools.

The use of SME involves the incorporation of a generic system dynamics model into a spatial array (similar to CA modeling), whereby the parameters of spatial data are used to create a matrix of spatially specific system dynamics models. In contrast to system dynamics software such as STELLA, the installation and use of SME requires some technical expertise. This is due in part to its flexibility in working with different modeling platforms (such as STELLA, Vensim, Simulab, among others), its open-source nature, and its origins in the Linux operating system (tending to require users with higher levels of computer literacy).

This type of modeling has the potential to overcome the spatial limitations (massive complexity in creating spatial models) of pure system dynamics, while still harnessing the educational features and policy formation benefits of representing system feedback explicitly. With the increasing availability of high quality remote sensing data, geographic information systems (GIS) and the development of parallel computer systems, limitations once placed on modeling systems by computer speed and input data requirements have begun to erode (Maxwell and Costanza, 1997). High data requirements and complex computational processes slow model development and implementation. This method of highly abstracting technical details allows for a focus on model communication that sets SME apart from standard CA modeling practices, while a focus on spatially explicit modeling sets it apart from the standard system dynamics practice of aggregation.

Development of the dynamic model of the EABs spread through host ash tree landscapes began with the parallel development of EAB and ash tree sub-models. These sub-models are linked through the parasitic relationship in which live ash bark area acts as habitat for EAB larvae. The EAB larvae act to consume live ash trees, reducing available bark area, increasing EAB density and necessitating the spatial spread of adults. For the creation of this model, we utilized the STELLA® iconographic modeling software (for a description of STELLA®, see Costanza and Voinov, 2001).

The combination of STELLA and SME modeling platforms allows for the integration of dynamic and spatial modeling techniques. This contrasts with purely dynamic models that have limited spatial orientation (such as Mack et al., 1987), as well as spatial models that tend to be more static (Zhao et al., 2006). Several other notable models of invasive species spread have attempted to integrate spatial and temporal modeling (Welk, 2004; Reeves and Usher, 1989). However, many of these models do not combine population growth rates and interactions with spatial diffusion. Rather, many models use ingenuous methods of simulating growth exogenously, such as genetic algorithms (Mau-Crimmins et al., 2006; Welk, 2004). We assert that the use of realistic, high-resolution landscape data is an important factor leading to the eventual use of models as predictors of spatial spread patterns (and eventual tools for slowing spread). This modeling project uses high-resolution landscape data, as compared to theoretical landscapes such as those shown in Legaspi et al. (1998), and low-resolution data such as the counties modeled in Stoker et al. (1994).

3.3. *EAB population model*

3.3.1. *EAB life cycle*

For the purposes of this model, we abstracted the insect life cycle as distinct, non-overlapping stages covering a 52-week period (Fig. 3).[3] The EABs egg stage is incorporated into the adult stage of lifecycle as an extra month. Females are assumed to lay an average of 78 eggs over 6 weeks (or 13 eggs per time step/week; near the upper bound of the range estimated by McCullough and Katovich (2004)) (Yiguo, 1966). Fig. 4 illustrates the translation of the EAB lifecycle into a

[3] In the model, 1 week is equivalent to one time step.

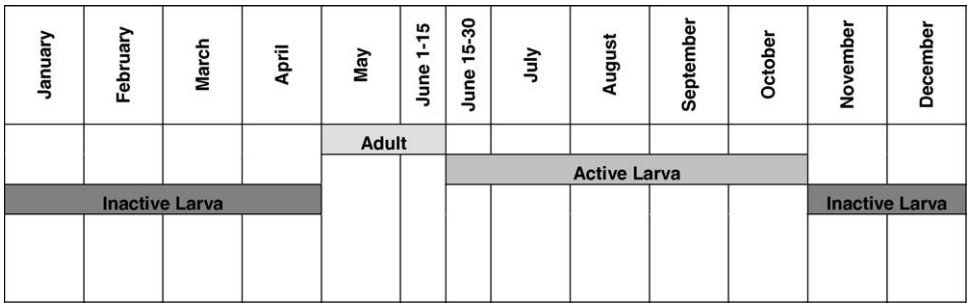

Fig. 3 – Model abstraction of Emerald Ash Borer lifecycle.

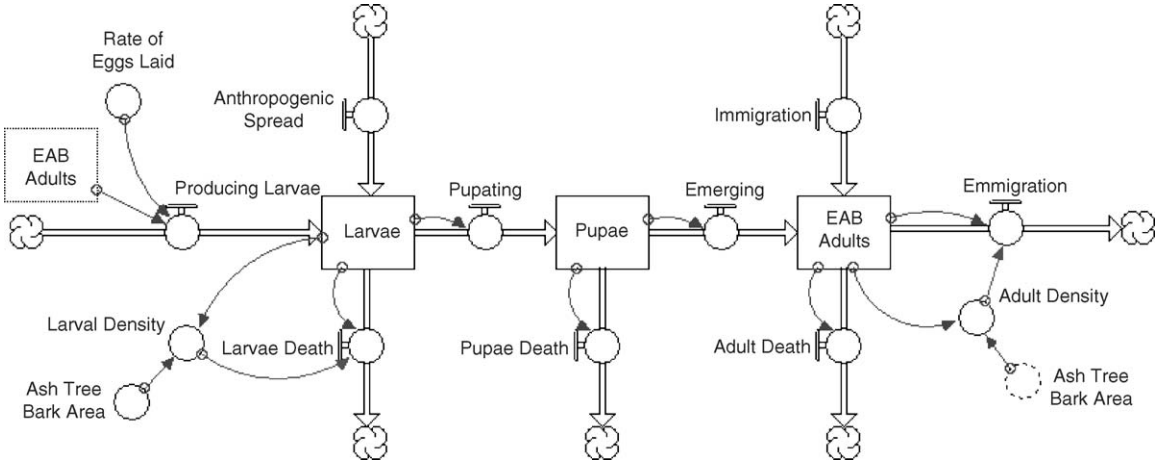

Fig. 4 – Stock-flow diagram simulating EAB lifecycle dynamics.

STELLA stock-flow diagram. These dynamics are contained within a single grid cell as replicated in the spatial modeling environment.

EAB larvae are modeled as actively feeding on ash trees for 20 weeks, from mid-June through the end of October. As the density of larvae increases, so does their death rate (Fig. 5). The maximum larval density is assumed to be 300 individuals per square meter of bark surface area (McCullough et al., 2003).

Deaths at the larval stage occur due to density dependency, where density is the number of larvae per total tree bark area

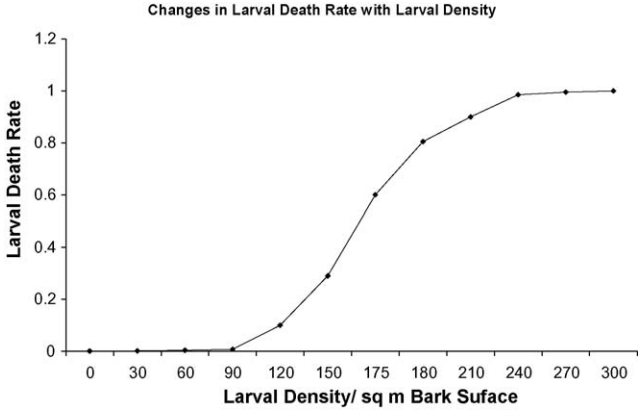

Fig. 5 – Larvae death rate as a function of larvae density.

in a cell. The nature of this relationship has yet to be captured in the literature, and therefore we assume a convex relationship between larval density and death rate. The relationship is assumed to be non-linear, with a logistic inflection point at 220 larvae/m^2 bark area (death rate is 40%) and a potential maximum 100% death rate at 300 larvae/m^2 (this death rate is never actually achieved in the model due to the rapid die-off of EAB larvae at near-maximum densities).

Inactive larvae and pupae are represented during a 22-week inactive period lasting November through April. EAB larvae have a winter diapause due temperature decreases. During this diapause, feeding ceases, and larval impact on tree health is halted. Feeding also halts during the EAB pupae stage. The density of inactive larvae is based on the number of active larvae and death rate of inactive larvae. The death rate of inactive larvae is assumed constant at 0.5% of the population per week, such that approximately 11% of pupae would die over the course of the inactive stage. Pupal and inactive larvae deaths are modeled to be the result of predation and harsh environmental conditions. No additional density dependence considerations need to be included during this stage since increased death rates for high-density clusters have already been captured for the larval stage.

Adults are set to live for six time steps from May through June 15th (Lyons et al., 2003). The maximum density of EAB that emerge as adults (M:F sex ratio is 1:1; Lyons et al., 2003)

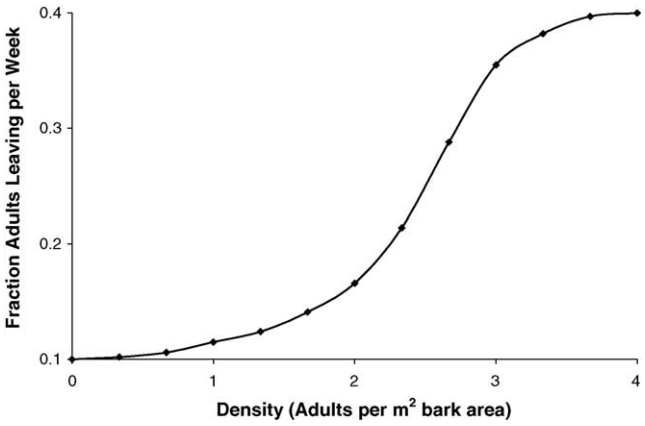

Fig. 6 – Fraction EAB adults leaving per week.

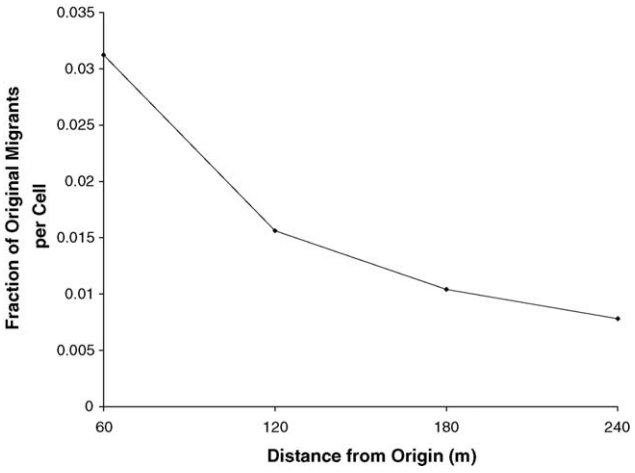

Fig. 7 – EAB migration fraction.

is set at 4 individuals per square meter of bark area.[4] Adult density is dependent upon the number of adults immigrating into the cell, and the number of adults dying. A delay of 6 weeks is incorporated to account for the natural life span of the adult. Predation from birds, etc. is considered to be insignificant.

3.3.2. *EAB distribution*

The spatial dynamics of the EAB lifecycle take place during the adult stage when they take flight in order to find mates and proper host trees for oviposition. Here, immigration and emigration from the 60 m cell dominate the EABs' egg-laying behavior and determine egg-laying distribution patterns. We consider here that the fraction of adult EABs leaving a given cell is again dependent on population density. In this case, we estimate an upper bound on adult density to be approximately 4 adults/m^2 bark area. A linear relationship is assumed for the adult emigration fraction with respect to population density, from 10% per week (50% per year) at the minimum without density constraints to 40% per week (95% per year) at the maximum (McCullough et al., 2003). Between this minimum and maximum, we assume the emigration rate follows an s-shaped curve, which levels out as it approaches the maximum density (Fig. 6).[5] Adult emigration is restricted to the time steps in which adults are present (weeks 18–24). Adults spatially migrate and lay eggs for a period of 6 weeks.

We assumed that the decision whether to migrate is dependent upon the density of the adults present in the cell and the total area of tree bark in the cell (Fig. 7). The distance the adult female is able to fly between cells limits migration distances. The emigrating EABs travel up to 240 m away from their origin during a week. This estimate was based on observations of females traveling 71–2426 m in 1 month (Bauer et al., 2003b). Since egg-laying takes place over a 6-week period, we estimate that the EAB may travel up to 1440 m over the course of its adulthood (Bauer et al., 2003b). This distance may be conservative, based on studies that indicate rare cases where potential travel distances may range as far as 2426 m (Bauer et al., 2003b).

The fraction of adults leaving an origin cell (i) for a destination cell (j) is defined by Eq. (1) below. This relationship underlies the asymptotically declining migration fraction utilizing the density-dependent function for adults leaving (Fig. 6):

$$B_{i\to j} = B_i \left(\frac{1}{r}\right) \frac{F(\rho_i)}{n y_{i\to j}} \tag{1}$$

where $B_{i\to j}$ is the number of EAB adults migrating from cell i to cell j, B_i is the number of EAB adults in origin cell i, $F(\rho_i)$ is the fraction of adults leaving cell i as a function of EAB adult density ρ (Fig. 5), n is the number of immediate neighbors surrounding cell i, eight neighbors (Moore neighborhood—see Wolfram, 1994), $y_{i\to j}$ is the shortest cell distance to destination cell j from origin cell i and r is the total number of migration rings defined by cell distance y from cell i, four rings.

Larval and adult densities are calculated by dividing their populations by the total tree bark area within the cell. This tree bark area is calculated by abstracting the tree trunk into a cylinder, and averaging the different heights and diameters of different age cohorts (Table 1).

Eq. (2) below illustrates the calculation of tree bark area:

$$A_j = \sum_i A_{ij}, \qquad A_{ij} = \pi d_i h_i T_{ij} \tag{2}$$

where A_j is the total tree bark surface area within cell j and age cohort i (m^2); i is the one of four susceptible tree age cohorts (10–20, 20–40, 40–75, 75+ years), j is the specific 60 m × 60 m cell defining location, d_i is the average diameter at breast height (DBH) of tree trunks in age cohort i (m), h_i is the average height of tree specific to age cohort i (m) and T_{ij} the total trees of age cohort i located in cell j.

[4] This estimation was derived from William Ruesinck (2004, personal communication).

[5] It should be noted that this curve represents a hypothetical relationship based upon available professional knowledge. However, aggregation effects of EAB on host trees may shift this curve towards the right, requiring higher densities to induce outmigration.

Table 1 – Ash tree size, seed production, and susceptibility to EAB larval infestation

Parameter	10–20 years	20–40 years	40–75 years	75+ years
Diameter at breast height (d_i)	0.075	0.18	0.3	0.43
Height (h_i)	5.5	17	23	27
Annual seeds produced	N/A	1.3 million	975000	600000
Larvae needed to kill tree (αA_{ij})[a]	65	481	1084	1824

Source: adapted from data in Burns and Honkala (1990).
[a] Larvae needed to kill tree is calculated as 50 borers/m^2 multiplied by tree bark area (A_{ij}).

3.4. *Tree population model*

3.4.1. *Tree life cycle*

In order to represent *Fraxinus* species in a model of EAB spatial spread, major simplifications were made by abstracting the three species commonly attacked by the EAB into a single species. This model simplification is possible if we assume that the EAB attacks each of the three species at equal rates. Under the flexible modeling framework used here, this assumption can be relaxed, but only in the presence of increased availability of data and substantial computational power.

Under this simplification, we abstract the *Fraxinus* species using averages among the characteristics mentioned in the background section. In general, *Fraxinus* species live to be about 150-years old. Seeding begins after 20 years, with maximum seed production occurring around 40 years and a decline at year 125 (Schopmeyer, 1974). Ash species rarely dominate forest canopy and do not form pure stands (Burns and Honkala, 1990). Flowering in these species occurs in April and May. Seeds are contained in a single winged samara and are wind dispersed up to 200 m (Burns and Honkala, 1990). A high mast year occurs in one out of 3–5 years (1–8 years in the case of *F. nigra*, but we will assume that high mast seed yield occurs every 4 years). Seeds are used by waterfowl, birds, small mammals, and deer for food, but are not a large component of any of these animals' diets (Martin et al., 1951).

By age 10, *Fraxinus* species usually have grown to approximately 5 cm (2 in.) in diameter, the size commonly necessary for EAB infestation (Iverson et al., 1996). Kartesz (2004) estimated that urban ashes tend to live at least 60 years. Here, we estimate that they die off after approximately 75 years, while trees growing in non-urbanized areas live an average of 180 years. These assumptions are taken from averages in wilderness tree life expectancy for the *Fraxinus* spp. in Iverson et al. (1996).

We abstract the reproductive behavior of *Fraxinus* species by taking an average of the seeds produced by each tree in an average year. The average of the three *Fraxinus* spp. we are studying produces approximately 75 pounds of seeds with an average of 13,000 seeds per pound (Schopmeyer, 1974).[6] This yields an average of 975,000 seeds generated per ash tree per year in a non-mast year (mast years are simulated every 4 years with a four-fold increase in seed production).

In the model, we assume that *Fraxinus* species rarely germinate and grow by themselves in developed areas. Rather, we assume that newly introduced trees (assumed to be approximately 10-years old when planted) in urban areas will involve human intervention (planting regimes scheduled by park districts and urban foresters). In order to look at the complex stratification procedure necessary for *Fraxinus* germination, we simulate a seed bank with a land-use dependent germination rate (see Table 1). Seeds can stay viable in the seed bank for up to 5 years, each year encountering a lower germination rate (Burns and Honkala, 1990).

The tree lifecycle model looks at seed germination as a process by which viable seeds from a seed bank germinate. The lifecycle is considered in stages that differ significantly in terms of EAB susceptibility, seed production, and natural death rate. We treat ash trees under 10-years old that cannot produce seeds as insusceptible to EAB infestation due to their small diameter (Burns and Honkala, 1990; McCullough and Katovich, 2004). Trees between 10 and 20 years also do not produce seed, but are vulnerable to the EAB due to their tendency to have an average diameter larger than 5 cm (2 in.) (Burns and Honkala, 1990; McCullough and Katovich, 2004).

Normal ash tree death rates not influenced by the EAB are partly determined by a density dependency measure that incorporates competition and shading considerations. The model equilibrates around a maximum tree density that is derived from the assumptions for initial tree distribution. We make this assumption based on the rapid rate of urbanization seen over the last decade in DuPage County since the Nowak (1994) study, implying that the county's ash tree population is not likely to increase. Natural tree death rate is assumed to be an s-shaped function of population density (see Fig. 8), and grows to a maximal rate of 33% per year. Tree death rate due to EAB injury is a function of the number of larvae in the cell, as well as the time it takes larval infestations to mortally wound a tree. This delay period is empirically observed to be approximately 2.5 years on average as indicated by heavy canopy dieback (McCullough and Katovich, 2004). The adult EAB does feed on ash leaves, but the impact is considered insignificant (Bauer et al., 2003a). With these assumptions, tree death by EABs is described in Eq. (3) below:

$$DR_{ij} = T_{ij}\left(\frac{T_{ij}L_j}{\alpha A_{ij}\tau\sum_i T_{ij}}\right) \quad (3)$$

where DR_{ij} is the death rate of ash trees due to EAB in cell j and age cohort i (trees/year), L_j is the total active larvae in

[6] It should be noted that Schopmeyer (1974) gives these figures in terms of "cleaned" seeds. However, our analysis looks purely at the gross number of seeds, which therefore leaves out any consideration of seed density or weight. The values specifically for each species are 13,120 per pound for *F. americana*, 8100 per pound for *F. nigra*, and 17,260 per pound for *F. pennsylvanica*.

Table 2 – Ash distribution by land-cover category in DuPage County

Land-use code	Description	Grid cells	Ash per cell	Initial ash trees
21	Upland	15491	10	154910
44	Floodplain forest	1992	7	13944
25	Partial canopy/savannah	9039	5	45195
35	Urban open space	86322	5	431610
32	Low/medium density urban	90339	3	271017
31	High density urban	19899	1	19899
	Other land use	19574	0	0
	Total	242656		936575

Source: adapted from data collected by Luman et al. (2003) and Nowak (1994).

cell j, α is the EAB larvae density necessary for tree fatality (50 larvae/m^2), τ is the death delay due to EAB infestation, assumed to be 2.5 years, A_{ij} is the total tree bark surface area within cell j and age cohort i (m^2); i is the one of four susceptible tree age cohorts (10–20, 20–40, 40–75, 75+ years), T_{ij} is the total trees of age cohort i located in cell j and j is the specific 60 m × 60 m cell defining location.

3.4.2. *Ash distribution*

Data on the prevalence of ash trees (Nowak, 1994) and distribution of land-use types (Luman et al., 2003) in DuPage County were used to prepare digital raster GIS maps of the initial ash tree distribution. DuPage County was selected not only for its strong mix of urban and rural land-use types not seen in more highly urbanized counties in the region, but also due to its important economic and social relationships with Chicago's Cook County.

Nowak (1994) conducted a survey of urban forests in a study area encompassing the City of Chicago, Cook County, and suburban DuPage County. This survey incorporated detailed estimates of tree species by land-use, where land-use categories included institutional, residential, commercial, and vacant, among others. As these categories differ substantially from those defined in the Illinois Land Cover map (Luman et al., 2003), we utilized the Nowak (1994) data primarily for the aggregate ash tree estimates in DuPage County. Of the 14.9 million trees in DuPage County, green and white ash comprised an estimated 950,200 total trees, or 6.4% of the total tree-cover in the county (Nowak, 1994). Because DuPage County has been rapidly urbanizing and the estimated ash trees contained a wide standard error (±381,400 trees), we treated 950,200 as an upper bound in estimating the number of ash trees (Table 2).[7]

To determine environmental suitability for ash growth and to estimate ash density for each cell, we combined information from the Nowak (1994) inventory with the Land Cover of Illinois Database GIS data (Luman et al., 2003).[8] Remote sensing is tremendously useful in this capacity; however, assumptions and errors are inherent in categorizing remotely sensed data into land cover classes (see Table 3 on the following page for the 23 land cover classes used by the Land Cover of Illinois dataset).

The commonly used ESRI ArcGIS and ArcView software (ESRI, 1997; Ormsby et al., 2004) was used to prepare digital raster land-use maps of the study area composed of raster grid cells 30 m × 30 m. We chose a coarser spatial resolution of 60 m cells to decrease computational complexity and increase compatibility with ash seed dispersion and EAB flight behavior. The data set was thus converted from 30 m × 30 m grid cells to 60 m × 60 m grid cells, such that the processed cells were four times the size of the original cells (3600 m^2). This conversion process utilized ArcGIS algorithms that assigned land-use type to the coarser cells based upon relative dominance of constituent 30 m × 30 m land-use types.

When the process of adjusting the spatial resolution was complete, total cells for each land-use type were tallied. Ash density, defined as the number of ash trees per cell, was then estimated for relevant land-use types, such that the estimated ash total fell within the range of the Nowak (1994) estimate

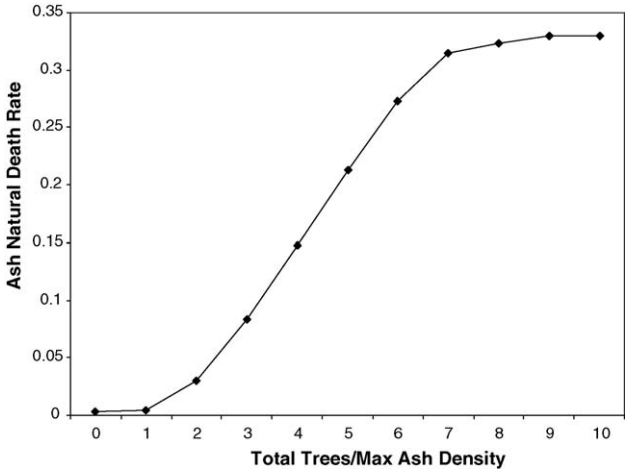

Fig. 8 – Ash natural death rate.

[7] The variation in this figure comes from high levels of spatial data aggregation in the Nowak (1994) study. Our goal was simply to establish a realistic and feasible tree distribution based on the upper and lower bounds given. It should be noted that a sensitivity analysis on this data was not performed, and represents an avenue for further research on this topic.

[8] The Illinois Interagency Landscape Classification Project (IILCP), comprised of the U.S. Department of Agriculture National Agricultural Statistics Service, the Illinois Department of Agriculture, and the Illinois Department of Natural Resources, began an initiative in 1999 to generate land cover data for the state of Illinois. This data is compiled using satellite imagery from Landsat 5 TM and Landsat 7 ETM+.

Table 3 – Land cover of Illinois dataset land classes

Agricultural land	Forested land	Urban land	Wetland	Other
Corn	Upland deciduous	High density	Shallow marsh/wet meadow	Surface water
Soybeans	Partial canopy/savannah	Low/medium density	Deep marsh	Barren and exposed land
Winter wheat	Upland coniferous	Urban open space	Seasonally/temporarily flooded	Clouds
Other small grains and hay			Floodplain forest	Cloud shadows
Winter wheat/soybeans			Swamp	
Other agriculture			Shallow water	
Rural grassland				

Source: adapted from Luman et al. (2003).

for ash trees in DuPage County. The Nowak (1994) estimates of percent tree cover, tree density and total trees by land-use type were integral to this estimate, although the land-use types were not aligned with the land-cover categories.

Nowak (1994) land-use types differed from the Illinois land-cover definition sufficiently that exact matches were not feasible. However, these categories were useful to guide the process of allocating trees to grid cells based upon Illinois land cover data. The Nowak (1994) land-use types included institutional buildings, transportation, agriculture, multi-residential, commercial/industrial, vacant, residential, and institutional vegetation. Forest preserves were identified as a land-use type but were not included in the Nowak (1994) estimates of urban forest structure.

The conceptual algorithm for ash tree allocation into individual land-uses involved distributing ash into the following land-use categories with decreasing frequency: uplands (highest rate), floodplain forests, partial canopy/savannah and urban open space, low/medium density urban, and high-density urban. Allocations were performed such that the total number of trees did not exceed the upper bound of 950,200 estimated ash trees (Nowak, 1994), under the logic that Dupage County's rapid pace of urbanization since the Nowak (1994) study would render higher tree counts unlikely (Table 2 outlines our assumptions for ash distribution for relevant land-use types from the land-cover of Illinois Database).

4. Results

After creating a homogenous test plot to ensure the proper functioning of the model, five simulations were performed. These model runs look at assumptions surrounding three different factors affecting the spread of the EAB: the landscape distribution of trees and land-uses, the ability of a county-wide firewood quarantine to effectively limit anthropogenically driven spread of the EAB, and the implementation of an eradication program similar to the Michigan Eradication Strategy (Michigan Department of Agriculture, 2003).

The tree distribution in the landscape was assumed to either be homogenous, where all cells contained the same number of trees, and therefore the same propensity for ash borer spread, or heterogeneous, where tree estimates were derived from Nowak (1994) and land-uses are given by data from Luman et al. (2003). Anthropogenic spread of the EAB was simulated through the introduction of EAB larvae in several cells spatially removed from the original introduction. These introductions were assumed to occur 3 years after the original infestation and take place in mid-May. This date was chosen because it occurs towards the beginning of the camping season, as camp ground firewood has been identified as a major vector of anthropogenic spread.

Finally, the eradication strategy simulated for the region mirrors that of the Michigan Eradication Strategy, which delineates the landscape into four major zones of consequence. The "core zone" is the area of known EAB infestation where the population will continue to infest ash until it has exhausted its resources, at which point the population will crash. The "suppression zone", a band bordering the core zone, is the area, which will soon host the natural spread of the EAB. This area acts as a buffer between the core zone and the firebreak zone since many parts may have already been slightly infected by

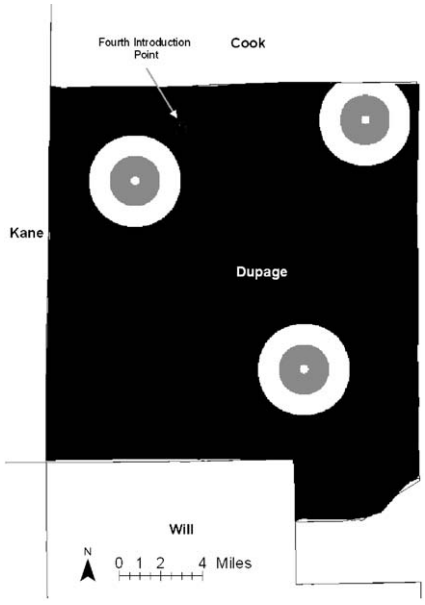

Fig. 9 – Introduction points and eradication strategy areas. The fourth, undetected introduction point is shown at the arrow tip. This introduction is made into an area with very few ash trees, thus slowing the ability of the borer to build up a high population for raid spread. The eradication zones are shown as concentric 1-mile bands around the perimeter of the known infection (large white dots in center of rings are infections after 3 years). Gray band: suppression zone (1-mile wide); white band: firebreak zone (1-mile wide).

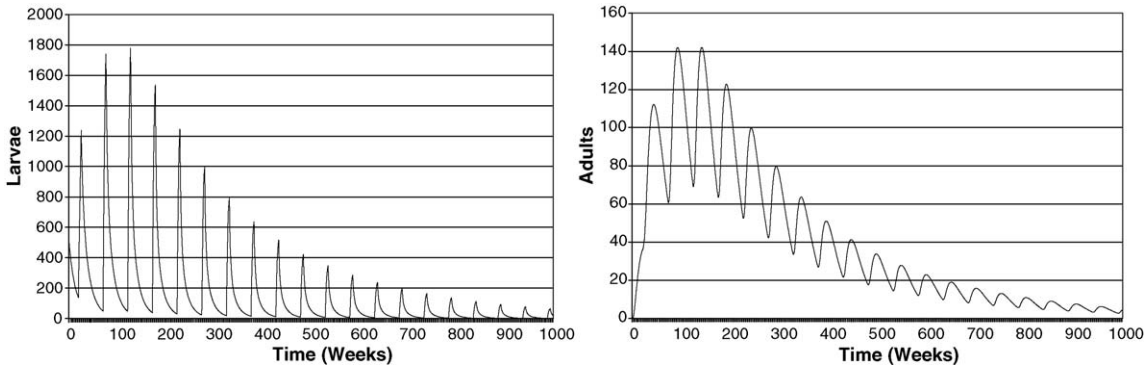

Fig. 10 – Individual cell overshoot and collapse of larval and adult populations.

fast-moving insects. Strategies for population density reduction in the suppression zone include both selective removal and chemical pesticide treatment of infested trees. Finally, the "firebreak" zone, another band surrounding the suppression zone, is meant to be an area free of ash trees that prevents the natural spread of EAB outside the known infested area. In addition to removal and/or treatment of isolated infestations, the preventative removal of all ash trees in this zone is meant to ensure that no hosts remain if further EAB spreading occurs outside of the suppression zone. The eradication strategy tested here implements the suppression and firebreak zones as 1-mile bands around the treated infestation sites. The concentric bands tested here are smaller than those proposed in the Michigan Eradication Strategy due to the relatively small size of our study area (the use of a 3-mile wide firebreak zone would envelop a huge portion of DuPage County). Fig. 9 shows the locations of infestation sites we simulated.[9] These four introductions involved the simultaneous introduction of 500 larvae into a single cell at each introduction location. This figure also illustrates the eradication strategy zones with the middle grey band representing the 1-mile-wide suppression zone, and the outer white band representing the 1-mile-wide firebreak zone.

The five model runs included:

(1) *Homogenous firewood quarantine*: uniform tree distribution with no anthropogenic spread.
(2) *Heterogeneous firewood quarantine*: realistic heterogeneous tree distribution with no anthropogenic spread.
(3) *Heterogeneous non-quarantine*: realistic heterogeneous tree distribution with anthropogenic spread represented as EAB introductions after initial infestation.
(4) *Eradication strategy and firewood quarantine*: realistic heterogeneous tree distribution with eradication strategy implemented roughly 3 years after original infestation (no anthropogenic spread).
(5) *Eradication strategy and no firewood quarantine*: realistic heterogeneous tree distribution with eradication strategy implemented roughly 3 years after original infestation. Anthropogenic spread is represented as EAB introductions after initial infestation and is not followed by any eradication strategy.

When turning off the EABs ability to spread to nearby areas, an overshoot and collapse behavior was detected in individual cells (see Fig. 10). Moreover, the model confirms empirical observations of oscillatory seasonal cycles of population density within individual cells (Bauer et al., 2003a; Lyons et al., 2003). Density-dependent feedback results in logistic growth and maintenance of adult population density (per bark surface area) throughout the population decline. The population and the host decline together, thereby maintaining density in a dynamic equilibrium. This density oscillates steadily between two bounds as seasons change (see Fig. 11).

Here, the dynamics of insect emigration and immigration from cell to cell show that EAB movement is necessitated by its cellular loss of carrying capacity due to its virulent behavior. In the first scenario, where a uniform initial distribution of host trees was simulated, the EAB spread pattern takes the form of expanding concentric rings. This is the result of evenly

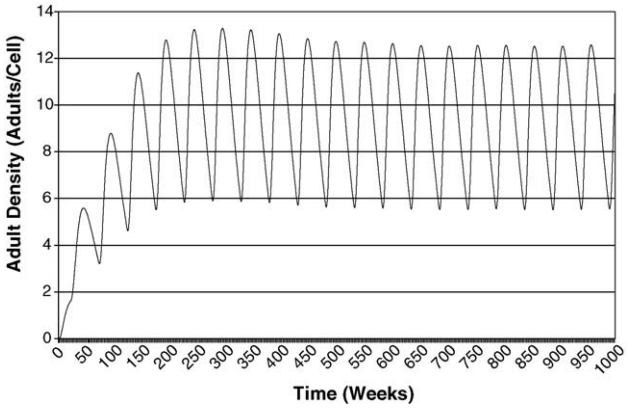

Fig. 11 – Seasonal oscillations in adult population density during population decline.

[9] Fig. 9 shows the infestations after 3 years for visualization purposes. The fourth infestation site marked with an arrow was placed in an area with very few trees. Here, we simulate a small infestation that future eradication strategies fail to address due to lack of detection.

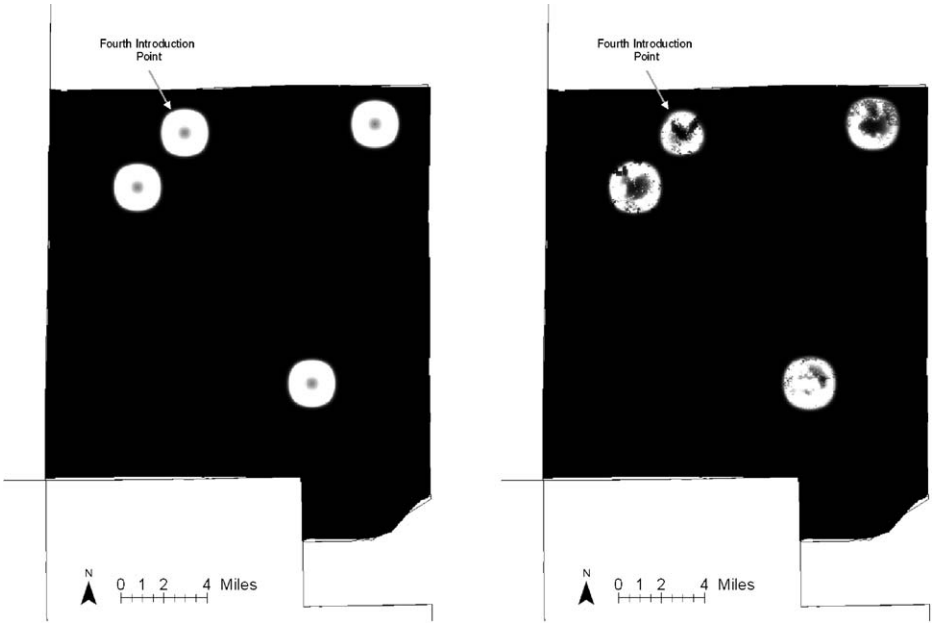

Fig. 12 – Comparison of adult spread rates in homogeneous and heterogeneous tree surfaces. Adult spread rates over homogenous (left) and heterogeneous tree surfaces (right) are similar. This is due to the propensity of the EAB to move faster through areas with fewer trees, which is balanced with the host carrying capacity of each cell. This carrying capacity limits the population growth of the EAB in any given year. The fractional values are the result of STELLAs tendency to model populations as continuous variables, rather than as discrete individuals. Both scenarios are shown during week 988.

distributed emigration due to high population densities and decreased carrying capacity.[10]

The model's structure suggests that in simulations using a heterogeneous tree distribution (informed by the land-use cover and host tree inventories), which contains a lower average number of trees, the insects would spread faster through the area. This is the direct result of high initial population densities in these areas, resulting in a high propensity for spatial dispersion.

However, the spread rates in the first two simulations are comparable (as shown in Fig. 12). This is due to the fact that the homogenous tree distribution in the first simulation contains a higher average number of trees than the heterogeneous distribution, thus facilitating a higher number of surviving larvae in each generation. Higher numbers of surviving larvae act to counteract the spread rate by quickly achieving the same density and population dispersion fraction seen in the heterogeneous map.

Although the assumed tree densities (0–10 per cell), spread capabilities (up to 1.4 km per year per insect), and necessary EAB larvae density for fatal tree damage (50/m^2) are all reasonable figures based on empirical evidence and professional estimations, the spread rates do not resemble those seen in infected areas in Michigan and Ontario, Canada.

To speed the spread of the EAB, the third simulation employs the same heterogeneous tree distribution as before, but fails to maintain a successful firewood quarantine. Fig. 13 shows the spread patterns resulting from three separate quarantine violations taking place 3 years after the initial infestation. These new EAB introductions take place in mid-May (week 175 of the simulation), the rough beginning of the summer outdoor recreational season. Here, we can gain significant insights into the EABs spread vectors by noting that this scenario simulates only three small anthropogenic introductions. This is significant since these introductions alone nearly double the EAB infestation area within 7 years. In areas in Michigan, the number of unique human introductions may number in the thousands, since quarantines were not implemented until 5–10 years after the original EAB introduction (McCullough and Katovich, 2004).

The fourth and fifth scenarios employ an eradication strategy similar to that of the Michigan Eradication Strategy. In the fourth simulation, the eradication strategy is coupled with a successful firewood quarantine, in which no new EAB introductions are made. The fifth simulation lacks a successful firewood quarantine, yielding new infestations of EAB that do not receive any eradication attention. These eradication programs are implemented exactly 3 years after the original infestations to simulate the delay associated with identifying EAB infestations and crafting the strategy for addressing it. Figs. 14 and 15 reveal the effects of successful eradication programs when combined with successful and non-successful firewood quarantine programs. The promising effects of this eradication strategy are depicted in Fig. 16, where the suppression and firebreak zones are overlaid on the adult spread map. Here, the suppression zone successfully reduces both the EAB larvae and adult population, while the 1-mile wide

[10] Prevailing winds are not considered in our analysis. Recommendations for inclusion of this factor in the EABs spread behavior are given in Section 5.

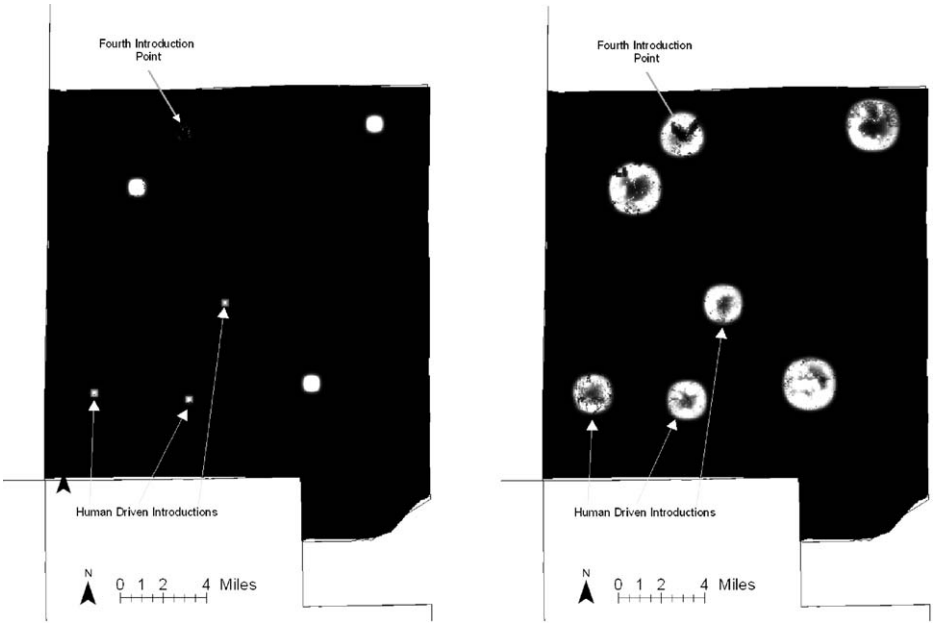

Fig. 13 – Adult spread map with unsuccessful firewood quarantine. New infestations are shown as they would appear a little over 3 years after they are introduced (week 364) and how they would appear after roughly 20 years (week 988). Anthropogenic introductions, as well as the fourth untreated introduction point, are shown with the arrows.

firebreak zone effectively ends the EABs spatial spread. The fourth, untreated introduction point successfully continues to spread, although spread within the firebreak zone is impossible since the zone has been rendered host-free.

The major insight emerging from this analysis is the role that effective firewood quarantines have on reducing the spatial spread of the borer. The eradication strategy simulated here effectively ends infestations, but damage from untreated human introductions continues unabated. Furthermore, the use of this two-step eradication technique for multiple infestations may begin to take a major toll on the area's ash tree population. In each individual infestation treatment, insecticides are applied to 4.4 square miles, while ash trees in 10.68 square miles are cut down. By our estimates, this could

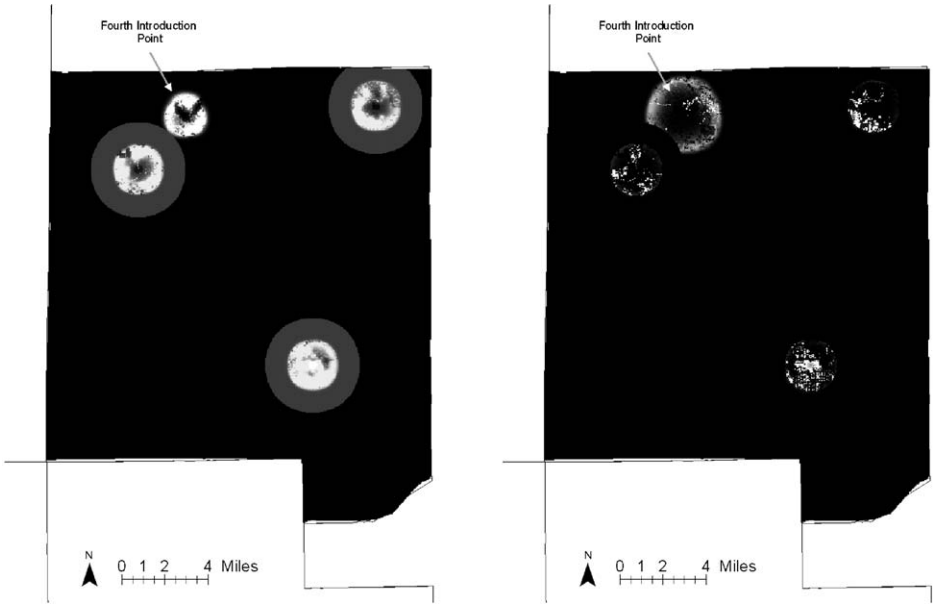

Fig. 14 – Adult spread map with eradication strategy and successful firewood quarantine. Adult spread map at week 988 (left), followed by adult spread map at week 1482 (right). The eradication strategy's firebreak zone is shown as the gray band surrounding the growing infestation area during week 988 (left).

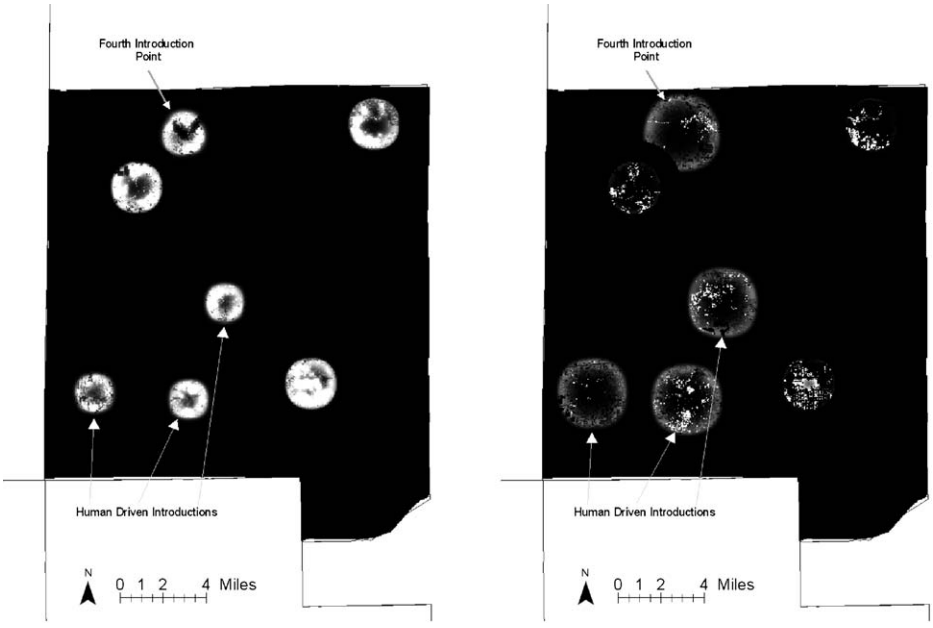

Fig. 15 – Adult spread map with eradication strategy and no firewood quarantine. Adult spread map with eradication strategy and failed firewood quarantine. Adult spread is shown during week 988 (left) and again at week 1482 (right). Anthropogenic introductions, as well as the fourth untreated introduction point, are shown with the arrows.

amount to upward of 76,000 trees cut down per infestation treatment, a major economic and aesthetic burden on state governments as well as local communities. Here, the role of quarantines presents itself as a particularly important focus for limiting future spreads.

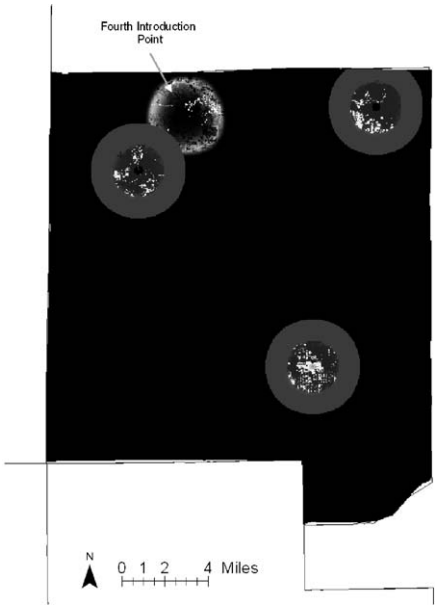

Fig. 16 – Blocked anthropogenic spread is due to eradication strategy's firebreak zone. The eradication strategy's firebreak zone is seen again limiting the spread of treated infestations during week 1482. However, the infestation at the fourth infection point remains untreated and continues to spread (note that its spread cannot enter into the host-free firebreak zone area).

5. Discussion and conclusions

The use of spatial dynamic modeling as a means for understanding the spread of the Emerald Ash Borer (EAB) has been useful for several reasons. By creating a framework for assembling known information about how the EAB spreads and how the populations of the EAB and susceptible ash hosts function and change over time, we can begin to create a comprehensive outline for understanding how to prevent its spread. Although work on the economic and socio-psychological effects of the EAB is still ongoing, the future severity of the EABs impact on the landscape is daunting.

The EAB is a particularly virulent parasite whose spread influence can be viewed in terms of density. The borer's degradation of its own carrying capacity necessitates its spread. Here, this model elucidates the extent to which the EAB depends upon space to survive. Each model cell experiences an irruption of EAB activity, after which the carrying capacity plummets and the EAB is forced to move on. The dynamics of this behavior are quite similar to that of the Kaibab Plateau deer herd, whose early 20th century population explosion was only limited by foliage (Ford, 1999).

Recently developed simulation technology allows us to concurrently test wide varieties of scenarios in order to establish efficient and effective policies for limiting the damaging spread of this invasive insect. This study has suggested that the ability of firewood quarantines to successfully limit the spread of the EAB is paramount to limiting its destruction of susceptible ash trees. The operational success of such quarantines would require substantial efforts in enforcement (via penalties) and public awareness (via marketing). For the purpose of the model, we have assumed that such quarantines are operationally effective.

As shown in the first two simulations, the natural spread rate of the EAB is relatively slow when compared to situations where humans assist in widening the reach of the EAB. The capacity of anthropogenic spread in widening the reach of the EAB is evident when considering that the third simulation only includes three new points of human driven introduction. A more realistic scenario may find that hundreds of new introduction points are created every year, thus resulting in the blanket of infestation now seen throughout southeastern Michigan.

The policy insights that this model yields extend a measure of importance to the pesticide treatment of campfire and other transported wood vectors. This model shows quite explicitly that the first step in limiting the damage inflicted by the EAB is the implementation and strict enforcement of comprehensive firewood quarantine programs. Fig. 13 shows the damage that quarantine failures can inflict on the landscape, even in the face of otherwise-effective eradication policies. As mentioned above, the operational success of the quarantine derives from enforcement and public awareness. Evasion of quarantines by gathering firewood deep within forests could further undermine the strategy and promote further EAB spread. This model also demonstrates the importance of monitoring to ensure the early identification of EAB infestations. The eradication strategies implemented in scenarios four and five show the damage that EAB infestations can inflict, even when infestations are identified less than 3 years after they begin.[11]

In general, simulation strategies have been noted for their ability to foster insights that are not feasible to obtain through other research methods. Scenario-driven models can help to identify knowledge gaps and provide a framework for further empirical research and field surveys. Here, the modeling process proves to be as important as the model output. We suggest that spatial dynamic modeling of the EABs spread is a powerful and flexible mechanism for clarifying and operationalizing empirically assembled information on EAB population and spread dynamics.

Simulation modeling often opens the door for many avenues for future research. The first involves the implementation of greater biological detail in both the tree and EAB population models, including increased seed production of ashes under stress as well as the effects of EAB pheromones on migration behavior. The second involves the application of this framework to locations with small EAB infestations and high quality tree data in order to validate assumptions and calibrate spread rates. Furthermore, a detailed study of spread patterns occurring in the face of urban development (with the associated patterns of tree removal and disposal, often expressed as tree movement, along with associated infestations) may be a promising method of establishing a more realistic picture of the EABs ability to capitalize on human-driven vectors. An analysis of wind effects on EAB spread behavior could also lend significant improvements to this study. Finally, this research elicits a call for the collection of high quality tree distribution data. The knowledge of host location will become imperative in the fight against the EABs spread in coming years as the insect spreads to an increasing number of metropolitan areas. Many areas, including Chicago and Detroit, maintain susceptible ashes as a high proportion of their municipal street trees. EAB infestations in these areas will be particularly damaging due to the high density of affected trees as well as the soaring costs of tree removal and replanting.

[11] This is instructive since the Michigan EAB introduction was not identified until 5–10 years after its introduction (McCullough and Katovich, 2004).

Acknowledgements

We would like to thank Dr. Zhanli Sun, Jeff Terstriep, and Michael Woodley for their wonderful insights, technical instruction, and code implementation for SME. We would also like to thank Bob Haack, William Ruesinck, and David Cappaert for help on insect life cycle, as well as Edith Makra, Joe McCarthy, Tom Green and Herb Schroeder for help on ash tree distribution and impact information. We would also like to thank Beth McLennan for her assistance with composing the GIS figures for this article. Finally, we would like to acknowledge Charlie Helm, Robert Wiedenmann, and Francis Harty for helping us understand the important role that modeling can play in invasive species studies.

REFERENCES

Acock, B., Reynolds, J.F., 1990. Model structure and data base development. In: Dixon, R.K., Meldahl, R.S., Ruark, G.A., Warren, W.G. (Eds.), Process Modeling of Forest Growth Responses to Environmental Stress. Timber Press, Portland, Oregon.

Auclair, A.N.D., Fowler, G., Hennessey, M.K., Hogue, A.T.e.a., 2005. Assessment of the risk of introduction of *Anoplophora glabripennis* (Coleoptera: Cerambycidae) in municipal solid waste from the quarantine area of New York city to landfills outside of the quarantine area: pathway analysis of the risk of spread and establishment. J. Econ. Entomol. 98, 47–60.

Barter, G.W., 1957. Studies of the Bronze Birch Borer, *Agrilus anxius* Gory, in New Brunswick. Can. Entomol. 89, 12–36.

Bauer, L.S., Haack, R.A., Miller, D.L., Petrice, T.R., Liu, H., 2003a. Emerald Ash Borer life cycle. In: Mastro, V., Reardon, R. (Eds.), Abstracts of Emerald Ash Borer Research and Technology Development Meeting. Forest Health Technology Enterprise Team. USDA FHTET-2004-02.

Bauer, L.S., Miller, D.L., Taylor, R.A.J., Haack, R.A., 2003b. Flight potential of the Emerald Ash Borer. In: Mastro, V., Reardon, R. (Eds.), Abstracts of Emerald Ash Borer Research and Technology Development Meeting. Forest Health Technology Enterprise Team. USDA FHTET-2004-02.

Bjorkbom, J.C., 1979. Seed Production and Advance Regeneration in Allegheny Hardwood Forests. Upper Darby, Pennsylvania: U.S. Department of Agriculture, Forest Service, Northeastern Forest Experiment Station. Research Paper NE-435.

Brown-Rytlewski, D.E., Wilson, M.A., 2003. Tracking the emergence of Emerald Ash Borer adults. In: Mastro, V., Reardon, R. (Eds.), Abstracts of Emerald Ash Borer Research and Technology Development Meeting. Forest Health Technology Enterprise Team. USDA FHTET-2004-02.

Burns, R.M., Honkala, B.H. (Eds.), 1990. Silvics of North America: Hardwoods. Agriculture Handbook 654, vol. 2. U.S. Department of Agriculture, Forest Service, Washington, DC.

Chicago Bureau of Forestry, 1995. The State of Chicago's Street Trees: A Random Sample Inventory. City of Chicago

Department of Streets and Sanitation, Bureau of Forestry, Chicago, Illinois.
Costanza, R., Voinov, A., 2001. Modeling ecological and economic systems with STELLA: part III. Ecol. Model. 143, 1–7.
Deal, B., Farello, C., Lancaster, M., Kompare, T., Hannon, B., 2004. A dynamic model of the spatial spread of an infectious disease: the case of fox rabies in Illinois. In: Constanza, R., Voinov, A. (Eds.), Landscape Simulation Modeling: A Spatially Explicit, Dynamic Approach. Springer-Verlag, NY.
Erdmann, G.G., Crow, T.R., Peterson, R.M., Wilson, C.D., 1987. Managing Black Ash in the Lake States. St. Paul, MN: U.S. Department of Agriculture, Forest Service, North Central Forest Experiment Station. General Technical Report NC-115.
ESRI, 1997. Getting to Know ArcView GIS: The Geographic Information System (GIS) for Everyone. Geoinformation International, Cambridge, UK.
Fall, A., Fall, J., 2001. A domain-specific language for models of landscape dynamics. Ecol. Model. 141, 1–18.
Ford, A., 1999. Modeling the Environment: An Introduction to System Dynamics Modeling of Environmental Systems. Island Press, Washington, DC.
Forrester, J., 1969. Urban Dynamics. Pegasus Communications, Waltham, MA.
Forrester, J., 1972. World Dynamics. Pegasus Communications, Waltham, MA.
Guo, H.C., Liu, L., Huang, G.H., Fuller, G.A., Zou, R., Yin, Y.Y., 2001. A system dynamics approach for regional environmental planning and management: a study for the Lake Erhai basin. J. Environ. Manage. 61, 93–111.
Haack, R.A., Petrice, T.R., 2003. Emerald Ash Borer adult disperal. In: Mastro, V., Reardon, R. (Eds.), Abstracts of Emerald Ash Borer Research and Technology Development Meeting. Forest Health Technology Enterprise Team. USDA FHTET-2004-02.
Haack, R.A., Poland, T.M., 2002. Evolving management strategies for a recently discovered exotic forest pest: the pine shoot beetle, *Tomicus piniperda* (Coleoptera). Biol. Invas. 3, 307–322.
Haack, R.A., Jendek, E., Liu, H., Marchant, K.R., Petrice, T.R., Poland, T.M., Ye, H., 2002. The Emerald Ash Borer: a new exotic pest in North America. Newsl. Michigan Entomol. Soc. 41, 1–5.
Hall, C.A.S., Day, J.W., 1977. Ecosystem Modeling in Theory and Practice: An Introduction with Case Histories. University Press of Colorado, Boulder, CO.
Herms, D.A., Stone, A.K., Chatfield, J.A., 2004. Emerald Ash Borer: the beginning of the end of ash in North America? In: Chatfield, J.A., Draper, E.A., Mathers, H.M., Dyke, D.E., Bennett, P.J., Boggs, J.F. (Eds.), Ornamental Plants: Annual Reports and Research Reviews 2003. OARDC/OSU Extension Special Circular, 193, pp. 62–71.
Hibben, C.R., Silverborg, S.B., 1978. Severity and Causes of Ash Dieback. J. Arboricult. 4 (12), 274–279.
Hosie, R.C., 1969. Native Trees of Canada. Canadian Forestry Service, Department of Fisheries and Forestry, Ottawa, ON.
Iverson, L.R., Prasad, A., Scott, C.T., 1996. Preparation of forest inventory and analysis (FIA) and state soil geographic database (STATSGO) data for global change research in the Eastern United States. In: Horn, J., Birdsey, R, O'Brian, K. (Eds.), Proceedings of the 1995 Meeting of the Northern Global Change Program. Radnor, PA: U.S. Department of Agriculture, Forest Service, Northeastern Forest Experiment Station. General Technical Report NE-214, pp. 209–214.
Kartesz, J.T., 2004. A synonymized checklist and atlas with biological attributes for the vascular flora of the United States, Canada, and Greenland. In: Kartez, J.T., Meacham, C.A. (Eds.), Synthesis of the North American Flora. Biota of North America Program (BONAP), University of North Carolina, Chapel Hill, NC.
Legaspi, B.C., Allen, J.C., Brewster, C.C., Morales-Ramos, J.A., King, E.G., 1998. Areawide management of the cotton boll weevil: use of a spatio-temporal model in augmentative biological control. Ecol. Model. 110 (2), 151–164.
Levy, G.F., 1970. The phytosociology of northern Wisconsin upland openings. Am. Midl. Nat. 83, 213–237.
Luman, D., Tweddale, T., Bahnsen, B., Willis, P. 2003. Land Cover of Illinois 1999–2000. Illinois Department of Natural Resources: Illinois Natural History Survey and Illinois State Geological Survey. 1:100,000 Scale Raster Digital Data, Version 2.0.
Lyons, B.D., Jones, G.C., Wainio-Keizer, K., 2003. The biology and phenology of the Emerald Ash Borer, *Agrilus planipennis*. In: Mastro, V., Reardon, R. (Eds.), Abstracts of Emerald Ash Borer Research and Technology Development Meeting. Forest Health Technology Enterprise Team. USDA FHTET-2004-02.
Mack, T.P., Smith, J.W., Reed, R.B., 1987. A mathematical model of the population dynamics of the lesser cornstalk borer, *Elasmopalpus lignosellus*. Ecol. Model. 39 (3–4), 269–286.
Martin, A.C., Zim, H.S., Nelson, A.L., 1951. American Wildlife and Plants: A Guide to Wildlife Food Habits. Dover, NY.
Mau-Crimmins, T.M., Schussman, H.R., Geiger, E.L., 2006. Can the invaded range of a species be predicted sufficiently using only native-range data? Lehman lovegrass (*Eragrostis lehmanniana*) in the southwestern United States. Ecol. Model. 193 (3–4), 736–746.
Maxwell, T., Costanza, R., 1997. A language for modular spatio-temporal simulation. Ecol. Model. 103, 105–113.
McCullough, D.G., Katovich, S.A., 2004. Pest Alert: Emerald Ash Borer. United States Forest Service, Northeastern Area. NA-PR-02-04.
McCullough, D.G., Agius, A., Cappaert, D., Poland, T.M., Miller, D.L., Bauer, L.S., 2003. Host range and host preference of Emerald Ash Borer. In: Mastro, V., Reardon, R. (Eds.), Abstracts of Emerald Ash Borer Research and Technology Development Meeting. Forest Health Technology Enterprise Team. USDA FHTET-2004-02.
McPherson, E.G., Nowak, D.J., Heisler, G., Grimmond, S., Souch, C., Grant, R., Rowntree, R.A., 1997. Quantifying urban forest structure, function, and value: the Chicago urban forest climate project. Urban Ecosyst. 1, 49–61.
Michigan Department of Agriculture, 2003. Emerald Ash Borer: Michigan Eradication Strategy. Retrieved 18 September 2005, from http://www.michigan.gov/documents/MDA_EAB_Strategy_86341_7.pdf.
Millers, I., Shriner, D.S., Rizzo, D., 1989. History of Hardwood Decline in the Eastern United States. Bromall, PA: U.S. Department of Agriculture, Forest Service, Northeastern Forest Experiment Station. General Technical Report NE-126.
Nowak, D.J., 1994. Urban forest structure: the state of Chicago's urban forest. In: McPherson, E.G., Nowak, D.J., Rowntree, R.A. (Eds.), Chicago's Urban Forest Ecosystem: Results of the Chicago Urban Forest Climate Project. Radnor, PA: U.S. Department of Agriculture, Forest Service, Northeastern Forest Experiment Station. General Technical Report NE-186, pp. 3–18.
Ormsby, T., Napoleon, E., Burke, R., Feaster, L., Groessl, C., 2004. Getting to Know ArcGIS Desktop, 2nd ed. ESRI Press, Redlands, CA.
Reeves, S.A., Usher, M.B., 1989. Application of a diffusion model to the spread of invasive species: the coypu in Great Britain. Ecol. Model. 47 (3–4), 217–232.
Schlesinger, R.C., 1990. *Fraxinus americana* L. white ash. In: Burns, R.M., Honkala, B.H. (Eds.), Silvics of North America. Hardwoods. Agriculture Handbook 654, vol. 2. U.S.

Department of Agriculture, Forest Service, Washington, DC, pp. 333–338.
Schopmeyer, C.S., 1974. Seeds of Woody Plants in the United States. Agriculture Handbook 450. U.S. Department of Agriculture, Washington, DC.
Smith, G., Hurley, J.E., 2000. First North American record of the Palearctic species *Tetropium fuscum* (Fabricius) (Coleoptera: Cerambycidae). Coleopts. Bull. 54, 540.
Sterman, J.D., 2000. Business Dynamics: Systems Thinking and Modeling in a Complex World. Boston, MA, McGraw-Hill.
Stoker, R.L., Ferris, D.K., Grant, W.E., Folse, L.J., 1994. Simulating colonization by exotic species: a model of the red imported fire ant (*Solenopsis invicta*) in North America. Ecol. Model. 73 (3–4), 281–292.
Vines, R.A., 1960. Trees, Shrubs, and Woody Vines of the Southwest. University of Texas Press, Austin, TX.
Voinov, A., Costanza, R., Wainger, L., Boumans, R., Villa, F., Maxwell, T., Voinov, H., 1999. The Patuxent landscape model: integrated ecological economic modeling of a watershed. Environ. Model. Softw. 14, 473–491.
Wang, B.S.P., 1974. Tree-Seed Storage. Ottawa, ON: Department of the Environment, Canadian Forestry Service. Publication No. 1335.
Welk, E., 2004. Constraints in range predictions of invasive plant species due to non-equilibrium distribution patterns: purple loosestrife (*Lythrum salicaria*) in North America. Ecol. Model. 179 (4), 551–567.
Williams, A.B., 1936. The composition and dynamics of a beech-maple climax community. Ecol. Monogr. 6 (3), 318–408.
Wilson, M.A., 2004. Emerald Ash Borer (*Agrilus planipennis*) biology and behavior. In: Proceedings of the Midwest Emerald Ash Borer Symposium, Novi, MI.
Wolfram, S., 1994. Cellular Automata and Complexity. Addison-Wesley, Reading, MA.
Wright, J.W., 1959. Silvical Characteristics of Green Ash. U.S. Department of Agriculture, Forest Service, Northeastern Forest Experiment Station, Upper Darby, PA.
Yiguo, L., 1966. A study on the Ash Bupestrid Beetle, *Agrilus* sp., in Shenyang. Shenyang, Liaoning Province, China: The Shenyang Municipal Institute of Gardening-Forestry Service.
Zhao, C., Nan, Z., Cheng, G., Zhang, J., Feng, Z., 2006. GIS-assisted modelling of the spatial distribution of Qinghai spruce (*Picea crassifolia*) in the Qilian mountains, northwestern China based on biophysical parameters. Ecol. Model. 191 (3–4), 487–500.